# Evaluation of seismic potential in a longwall mine with massive sandstone roof under deep overburden: An update

Mark Van Dyke, NIOSH, Pittsburgh, PA
Ted Klemetti, NIOSH, Pittsburgh, PA
Zoheir Khademian, NIOSH Pittsburgh, PA
Joe Wickline, Coronado Global Resources Inc., Beckley, WV
Jake Beale, Pilot Geophysical LLC, Riner, VA

## Abstract

In 2016, a 3.7-ML magnitude event caused by mining activity occurred at a longwall mine in southwestern Virginia which was recorded by the United States Geological Survey (USGS) and felt by local residents. The event was the largest of its kind since a global mine design change by the operator was instituted in 2008 following three large events in 2005, 2006 and 2007 (3.4, 4.3, and 3.4, respectively). Two of the three pre-2008 events (2005 and 2007) damaged ventilation controls in the mine which fueled a mine fire. In 2016 the mine's management requested researchers from the National Institute for Occupational Safety and Health (NIOSH) to access geological data and determine what parameters could possibly lead to events of a magnitude of 1.0 ML or greater. Evaluation of 2,152 geological data points and modeling revealed three major geological factors in common with the majority of the 181 recorded +1.0 ML events from 2009 through 2016. Three levels of seismic potential were identified as follows:

- **Low potential (1.0+ ML):** overburden greater than 579 m.
- **Moderate potential (1.5+ ML):** overburden greater than 579.12 m and 6.1–12.2 m of sandstone within 15.24 m above the coal seam.
- **Elevated potential (3.0+ ML):** overburden greater than 579.12 m, 6.1–12.2 m of sandstone within 15.24 m above the coal seam, and caving height of less than 4.5 m above the coal seam.

These three factors were used to create a seismic forecast map that produced an accuracy of 74%–89% for 1.0 ML or greater events, 72% accuracy for 1.5 ML or greater events, and 100% accuracy for 3.0ML or greater events based on seismic history (Van Dyke et al., 2017).

The map was created to not only show how geological data can be combined to understand why a mining related seismic event occurred in a particular area, but how the map could be used to forecast potential seismic areas in future mining. This paper is an update to report the accuracy forecasting large seismic events in areas mined since the map was originally published in 2017 and how the map has helped improve miner safety and health based on its implementation.

New changes to the forecasting process include implementing a change to the moderate potential criteria to expand the sandstone thickness to 4.6–12.2 m and decreasing the location error from a 91 m buffer to a 10% (58 m) elevation error based on the first overburden thickness threshold of 579 m. Since the first seismic forecasting map was published, the map has correctly forecasted 54%–71% of 115 total 1.0–1.4 ML events, 69%-83% of 49 total 1.5–1.9 ML events, and 88% of 9 total 2.0 ML or above events in previously unmined areas.

## Background

A 3.7-ML seismic event caused by mining activity occurred at a longwall coal mine in southwestern Virginia in 2016. The event was recorded by the United States Geological Survey (USGS) and reported by local media and residents. Unfortunately, this was not the only large seismic event that was recorded due to mining in the area. Previous large events in 2005, 2006 and 2007 (measured at 3.4, 4.3, and 3.4, respectively), damaged ventilation controls, which also fueled fires in the 2005 and 2007 events. The 2005, 2006 and 2007 events prompted a change of the global mine design by the operator in 2008 and the installation of a mine-wide seismic network that consisted of seven seismic stations that were positioned around the current mining district. The 3.7-ML event was the largest of its kind since the mine design change, which prompted mine management to request assistance from the National Institute for Occupational Safety and Health (NIOSH) to determine what parameters could lead to seismic events with a magnitude of 1.0 ML or greater. NIOSH researchers discovered similar geological features leading to seismic events, which led to creating a forecasting map to project possible future seismically active areas due to mining activity based on historical data.

After a comparison of 2,152 geological data points that were composed of in-mine fiberscope observations, electronic logs, and gas wells versus the 181 recorded +1.0-ML events between 2009–2016, common themes began to emerge. The most apparent influence for seismic activity was the overburden thickness. Seismic activity can happen at virtually any thickness of overburden, but there was a significant increase of the frequency and magnitude of seismic events starting at 579 m. Areas that meet only the 579-m overburden criterion are labeled as low potential for seismic activity on the forecasting map. The next finding that led to increased seismic activity was the presence of thick sequences of sandstone, and geologic computer modeling assisted in determining the specific thickness and height above the coal seam that was required to commonly produce seismic activity based on the historical data. In addition to the 579-m overburden parameter, the majority of the +1.5-ML events occurred where the sandstone thickness was between 6.1–12.2 m within 15.2 m above the coal seam. Areas of the map where both the overburden and sandstone thickness criteria are met are labeled as moderate potential seismic areas. A final geologic factor to focus on for areas that could cause seismic events of 3.0 ML or greater is the addition of the factor of expected caving height from mining that is less than 4.5 m. More specific information of the development of the method of the forecasting map can be reviewed in previous papers (Van Dyke et al., 2017, 2022).

## Mine Layout

The longwall mine considered in this study is in Buchanan County, Virginia, and mines the Pocahontas No. 3 coal seam. Since the publishing of the first seismic forecasting paper (Van Dyke et al., 2017), the mine has mined in two areas: first was the East panels, followed by the finishing of the remaining areas of the Right panel district (see Figure 1). The East panels were mined in an east-to-west direction versus a south-to-north direction of the Right panels. Both East and Right panels are 213-m wide, and the length varies between 1,707–3,475 m. The East panels are longer due to a geologic anomaly encountered near the recovery areas of the Right panels. Since October of 2016, the mine has successfully mined 13 longwall panels.

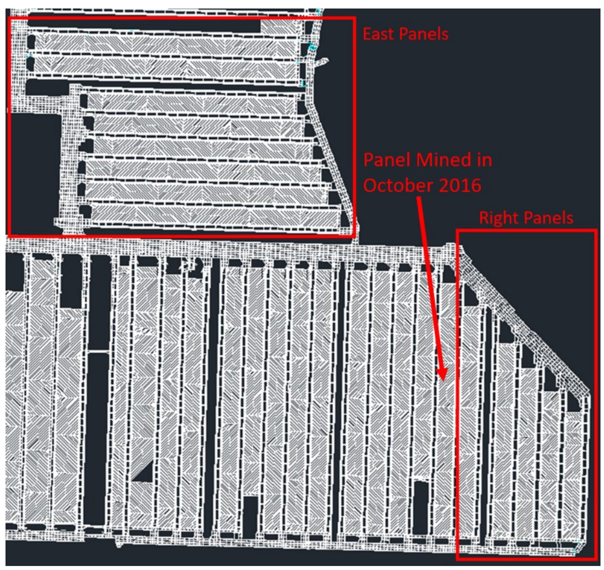

Figure 1. Mine layout in 2016.

## Seismic System

The 2016 seismic system consisted of seven surface stations that created an issue in determining the depth of the recorded events. To have better data control on the depth, two methods were tested to supplement the seven existing sensors as discussed in (Van Dyke et al., 2017, 2022).

The first method was to install three triaxial sensors up-hole into the roof of the mine. This method required using a 7.62 cm bit to drill into competent sandstone, which was between 4.5–6 m above the roofline. After the hole was drilled, the sensor was lifted and grouted into place. The grout was then pumped into the void until the grout exited out of the air vent tube. The underground system required a separate network than the surface network, and this caused issues when locating the events.

The second method was to lower a triaxial seismometer down 232 m into a gas well that was plugged with cement. This method was much less labor intensive and yielded immediate results since it was using the same network as the 7-sensor surface system. A further analysis of the two additional seismic systems is discussed in the next two sections.

**Three Underground Triaxial Seismometers**

Three underground seismic sensors placed in the sandstone just above mine level were incorporated into an existing network of seven sensors already operating at surface locations surrounding the activity of a longwall mine. Difficulty in meshing the underground arrival times with the above-ground arrival times for locating events was encountered, which may be due to an issue with the timing system (time-stamping of the data) of the underground stations, arising from an inability to properly synchronize the station clocks with the time server over a complex ethernet architecture. Although the three station clocks synchronized and appeared to be consistent from one station to another (see below discussion of low-quality locations using only data from these three stations), the overall timing appears to be offset from coordinated universal time (UTC) by a small, but meaningful amount.

Although the two datasets (surface arrivals and underground arrivals) have not yet been successfully meshed, many high-quality locations were obtained using only the manually picked, surface-station arrivals. Low-quality locations for about 800 of these events were obtained using arrivals from only the three underground stations. The better-constrained events show the expected trends along the mined panels and have a depth-distribution that is similar to that seen with higher-quality locations obtained from the surface system. The less-constrained events fan outward away from the area of station coverage as expected for event locations obtained from only three stations. This is seen in both map view and cross-section. The better-constrained event locations indicate that the timing provided to each of the underground stations was consistent, otherwise the arrivals would not have yielded meaningful event locations. An examination of the residual errors for the underground stations may yield enough information to allow for a correction to be made to their associated arrival times and facilitate incorporation of the two datasets. A thorough examination of the arrival time data will be necessary in order to resolve the discrepancy.

**Borehole Triaxial Seismometer**

After experiencing difficulty incorporating the underground seismic data into the existing surface seismic system, a borehole triaxial seismometer was installed in an area where the seven-station seismic network had been moved into a position surrounding ongoing longwall mining. In contrast to the approach taken with the underground seismic system in which two different data collection systems were operating and the data were then combined prior to event detection/location, the borehole seismometer was connected directly to an existing data collection unit within the surface seismic system. This eliminated the timing discrepancy that occurred with the underground seismometers. This approach also alleviated the difficulties encountered during the installation process and eliminated the effort that was needed to maintain a seismic system underground. The potential downside to this approach was that the borehole instrument would not be installed at mine level, but rather it would be installed significantly above mine level, although still well below the level of the surface stations. The borehole seismometer was installed at an elevation roughly 457 m above mining activity, beneath a surface station at an elevation roughly 701 m above mining activity.

Over 2,700 mining-related seismic events were recorded over a period of roughly 15 months, and P-wave arrival times were picked using a standard Short Term Average – Long Term Average (STA-LTA) picking algorithm (Withers et al., 1998). Multiple sets of event locations were produced using identical procedures: (1) a set using all available arrivals from both the surface network and the borehole seismometer; 2) a set using all surface arrivals and excluding arrivals from the borehole seismometer; 3) a set using arrivals from the borehole seismometer and all surface sensors except the sensor above the borehole sensor location. These results were qualitatively assessed using general criteria such as depth distribution and horizontal clustering. Experience has shown that the majority of the better-constrained events will cluster tightly with the long axis of the longwall panels and have a depth distribution within a hundred meters above mine level. It is then assumed that event locations more rigorously adhering to these criteria are, in aggregate, more accurate than those less clearly showing these characteristics.

For the purpose of showing the effect of including a station closer to mine level, reasonable estimates for average velocity of the entire volume were chosen based on prior analyses and limited investigation of a range of values. The average velocity value was then used for calculating travel times to surface stations for all events. Seismic velocity in the mining area tends to be slower in the upper part of the overburden above mining activity than it is in the lower part; therefore, a faster velocity was used to calculate travel times to the borehole seismometer than that used for calculating travel times to the surface seismometers.

When comparing the event location sets (see Figure 2), the set including all arrivals shows a marked improvement over the set excluding the borehole both in tight clustering and proper depth distribution. The along-panel distributions significantly tightened and moved closer to the tailgate edge of the associated panels. It is possible that some of this lateral movement could be an effect of using the wrong velocity for travel times at the borehole sensor, but this would not account for the improved clustering. The all-arrivals event locations also show improved clustering in depth. Many events that were located in the shallow section without the borehole arrival were, after its inclusion, shifted downward into the main clusters above the longwall panels. This depth distribution more closely matches expectation, and the downward shift of many locations was also accompanied by a small, lateral shift which, as noted above, tightened the horizontal clustering along panels, further suggesting that these locations are improved. To rule out the possibility that the improvement in locations was simply due to the addition of an extra sensor, the events were also located with the borehole arrivals but without the arrivals from the surface sensor above it (effectively replacing the surface sensor with the borehole sensor).

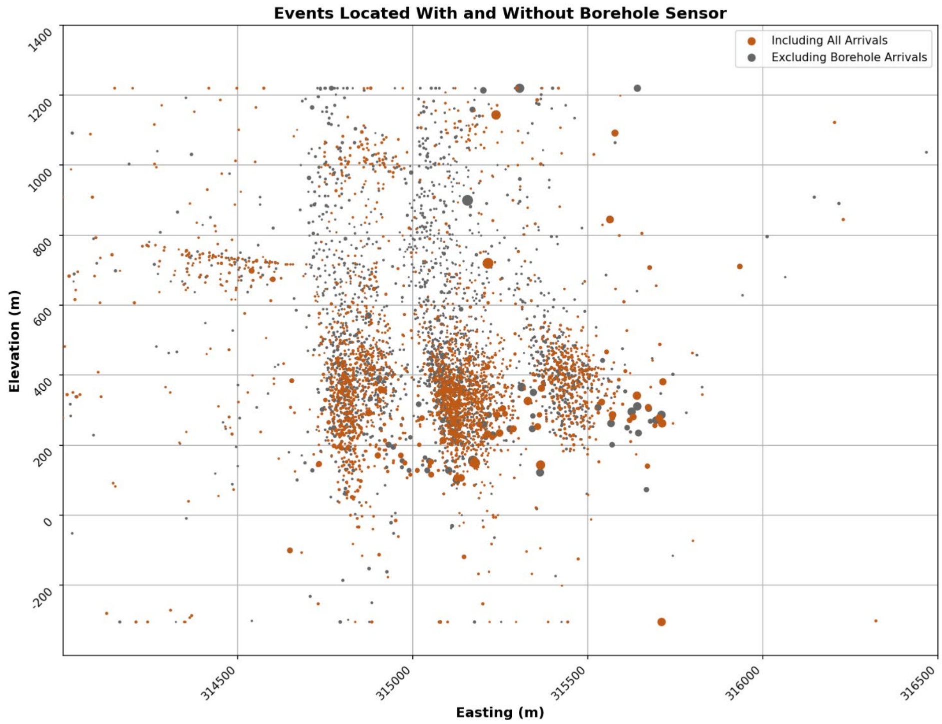


Figure 2. Cross-sectional view of seismic events.

While these results are qualitative, they do show an improvement due to the inclusion of a single sensor at a depth nearer to the region of highest seismic activity. In order to determine the optimum placement of such a sensor as well as other similar concerns, these results need to be more closely examined, and the effect of the borehole sensor on a variety of relevant parameters needs to be determined.

## Mine Geology

The Pocahontas No. 3 coal seam has favorable properties for coke production due to the high carbon and low impurities content. The seam is stratigraphically located within the Lower Pennsylvanian Series of the Pocahontas formation. The formation averages 213 to 274-m thick and contains sequences of upper deltaic deposits of massive sandstones, thin shales, clays, and coal. The mining area is within the Appalachian Plateau and Valley and Ridge physiographic provinces, which are characterized by rolling mountain ranges that typically trend in a northeast-southwest direction with alternating synclines and anticlines. Thrust faults are common in the area, but only the strike-slip Keen Mountain fault is close enough to have an impact on the mine's early history. The fault caused localized thrust faulting within the mine resulting in thinning and thickening sequences of the coal seam, which has small impacts on mining (Su et al., 2014; Van Dyke, 2017).

The near-seam mine geology (see Figure 3) consists of a floor sandstone that the mine has named the "sandstone floor" or SSF which can be 6 m or greater in thickness. Above the SSF and directly below the coal seam is a fireclay that averages 0 to 1.5-m thick that can cause floor heave issues in areas with thicker overburden. The next lithologic unit is the Pocahontas No. 3 coal seam, which averages 1.5 to 2.4-m thick. The immediate roof is a silty shale that averages 0 to 7.6-m thick and can contain laminations of coal or sandstone streaks. Above the silty shale is the first sandstone unit named "sandstone one" or SS1 by the mine. The SS1 averages 0 to 10.7-m in thickness and can be thinly to medium bedded with rare cases of massive bedding. Between the SS1 and sandstone 2 (SS2) is a shale parting that averages 0 to 1.5-m in thickness. In limited areas of the mine, the shale parting is absent and the SS1 and SS2 are combined. SS2 is medium to massive bedded and averages 9.1 to 22.9-m thick. The final unit in the immediate roof is the Pocahontas No. 4 seam which is 0 to 0.6-m thick.

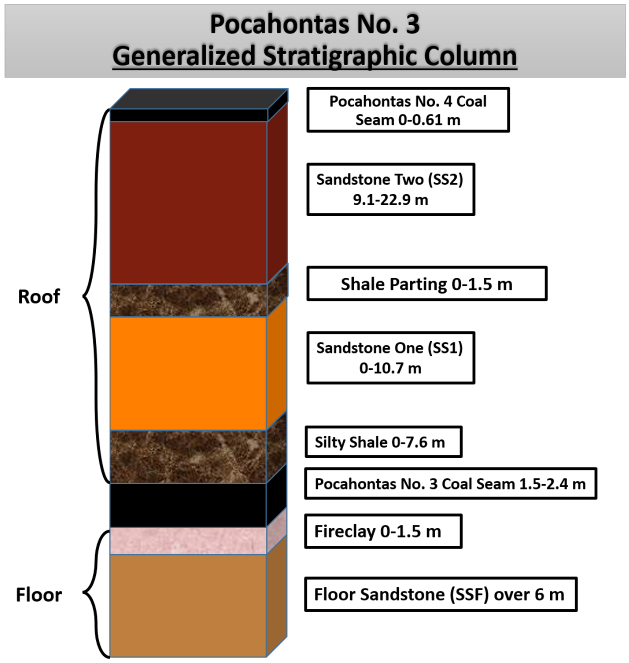


Figure 3. Generalized stratigraphic column.
(edited from Van Dyke et al., 2018)

**East Panel Geology**

The Eastern panel district's overburden differs from the Right panel district by having generally shallower overburden thicknesses (see Figure 4). A valley cuts through the middle of the panels and overburden thicknesses were measured to be below 366 m in thickness, but ridges on the longwall startup and recovery areas experience 610–732 m of overburden thickness. Due to the valley, much of the mid-panel areas does not meet the 579-m overburden low seismic potential criteria.

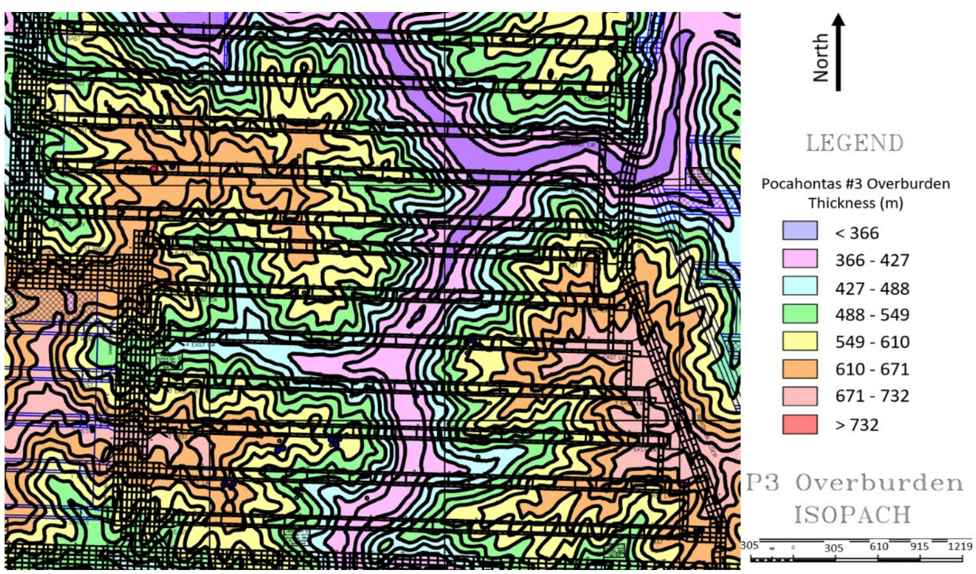


Figure 4. Overburden map of the Eastern panels.

The first sandstone (SS1) and second sandstone (SS2) are generally higher up from the roofline when compared to the Right panels. The SS1 and SS2 thicken at the longwall startup and longwall recovery areas and lift up from the seam mid-panel. However, there are areas that meet the moderate seismic potential criteria of overburden thickness greater than 579 m and 6.1 to 12.2 m of sandstone within the first 15 m of strata above the roofline (see figure 5).

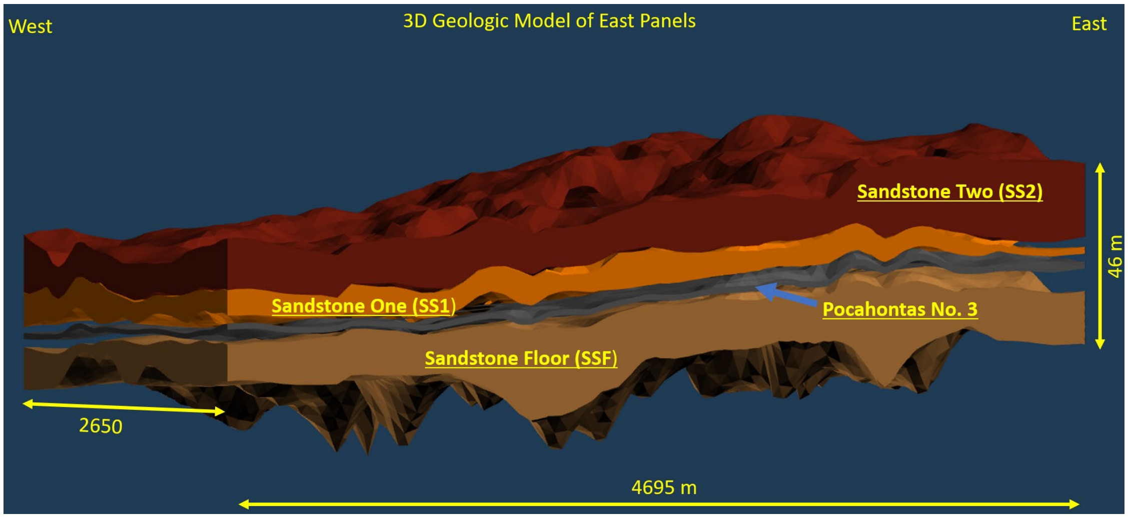

Figure 5. Modeled geology of the East panels.

**Seismicity of the East Panels**

In the East panels, a total of 9 longwall panels were mined in two districts separated by a barrier pillar. The first district contained 6 panels in which little seismic activity was expected mid-panel due to the thinning of the sandstone, better caving, and thinner overburden. Within a 5–6 panel district, typically the most seismic activity occurs at panels 3 and 4 (depending on the geologic parameters) due to being the furthest areas away from a coal barrier. Currently, geometric design, stress flow and speed of mining factors are not incorporated into the forecasting but may be incorporated in future versions. However, the number of seismic events in 1 and 2 East was much higher than experienced in the past Right panels. Overall, the forecasting map accurately forecasted 16 out of 47 (34%) total +1.0 ML events. The accuracy increases to 8 of 16 (50%) when forecasting events at 1.5–1.9 ML. In forecasting events of 2.0 ML or higher, the map correctly forecasted 1 of 1 (100%) event correctly. The total accuracy is heavily influenced by events in the 1.0–1.4 ML range. Smaller events are more difficult to forecast due to the increasing variability of factors that could not be foreseen unless an unpractical amount of geologic data was collected (see Figure 6).

In the first seismic forecasting paper (Van Dyke et al. 2017), a 91-m buffer was placed around each event to allow for location accuracy. In this study, the 91-m buffer has been replaced with a stricter 58 m (10% of the 579 m overburden criteria) buffer in the overburden thickness requirement to account for seismic location accuracy. The majority of incorrectly forecasted seismic events were due to missing the elevation requirement. When adding the 58 m buffer to account for forecasting accuracy, the total number of correctly forecasted events from 1.0–1.4 ML raises from 34% to 61.7%. The 1.5–1.9 ML event forecasting rate increased to 87.5%, and the single 2.0+ ML event was again correctly forecasted (see Table 1). As additional seismic and geologic data was collected it was determined that the second requirement (sandstone thickness) to determine moderate seismic potential needed to be expanded slightly. Seismic events between 1.5-3.0 ML were occurring in thinner sandstones than the original range of 6-12 m. The range of sandstone thickness within the first 15 m of roof was changed to 4.5-12 m to better reflect the new data.

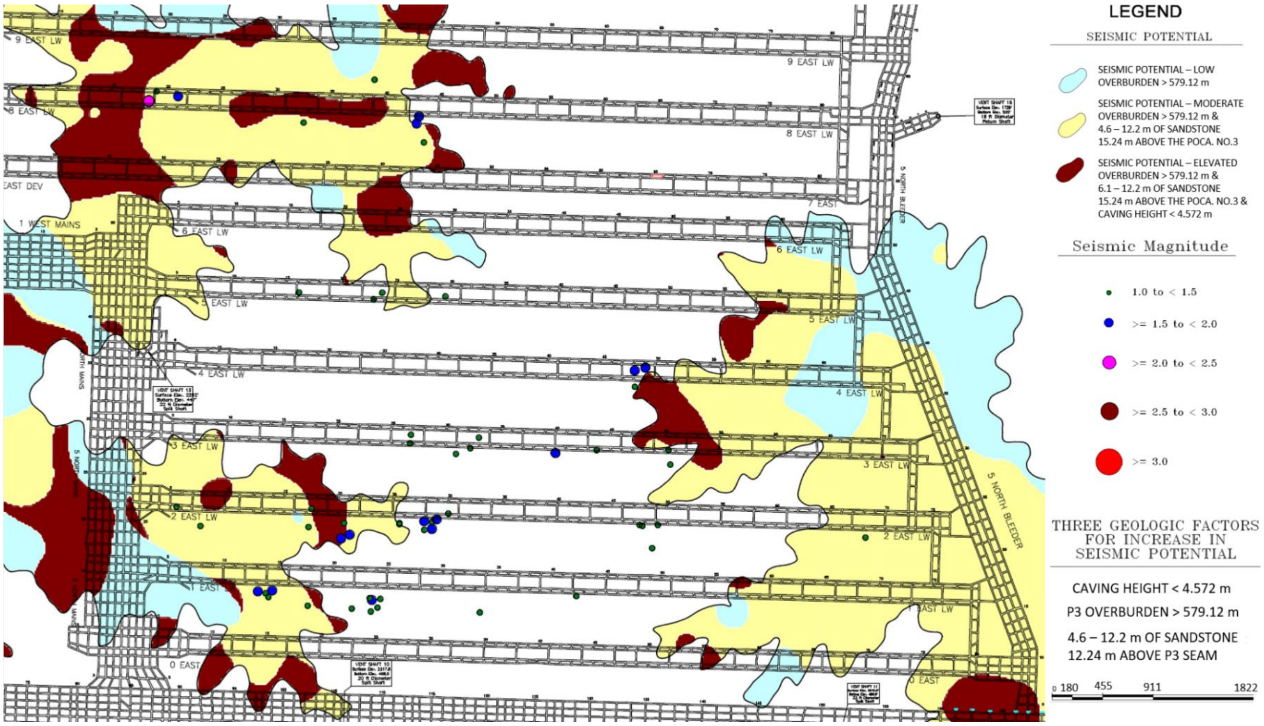


Figure 6. Seismic potential map of the East panels.

Table 1. Forecasting accuracy of the East panels.

| East Panels Seismic Potential Event Accuracy | | | | | | | |
|---|---|---|---|---|---|---|---|
| No Correction | | | | 10% Elevation Bump for Location Error | | | |
| **Event** | **Predicted** | **Total** | **% Correct** | **Event** | **Predicted** | **Total** | **% Correct** |
| **1.0–1.49 ML** | 16 | 47 | 34.0% | **1.0–1.49 ML** | 29 | 47 | 61.7% |
| **1.5–1.99** | 8 | 16 | 50.0% | **1.5–1.99** | 14 | 16 | 87.5% |
| **2.0–2.99** | 1 | 1 | 100.0% | **2.0–2.99** | 1 | 1 | 100.0% |
| **3.0+** | 0 | 0 | - | **3.0+** | 0 | 0 | - |
| **Total** | 25 | 64 | 39.0% | **Total** | 44 | 64 | 68.7% |

## Right Panel Geology

The Right panel district encountered some of the deepest overburden to date peaking at 700 m. A narrow valley cuts across the panels from east to west and impacts each panel differently because of a change in mine geometry. Deep cover exists in the backend across all the panels where large portions of several panels meet the 579-m overburden criteria (see Figure 7). The flank of the Dry Fork Anticline was encountered in the very southeast area of the last panel in the district, which seemed to relieve seismic activity, but caused an increase in methane content during mining.

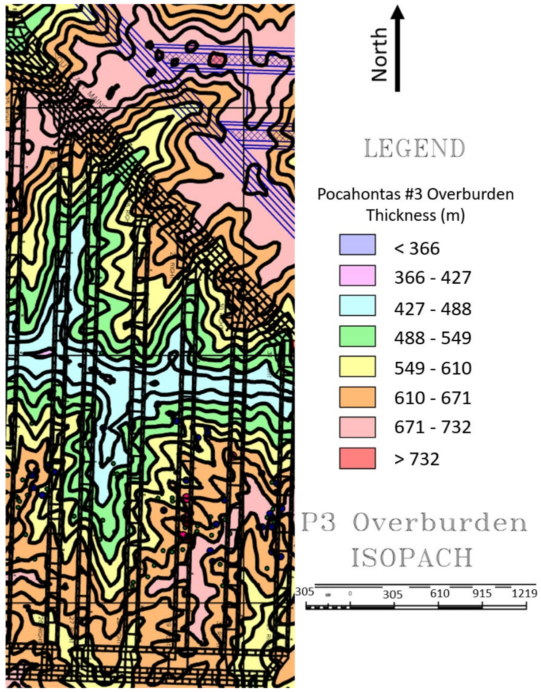


Figure 7. Overburden thickness map for the Right panels.

The SS1 and SS2 sandstone units are generally thicker in the Right panels compared to the East panels. The average thicknesses of SS1 and SS2 units for the Right panels are 7.3 m and 19.8 m compared to 5.9 m and 10.3 m in the East panels. The shale parting between the two units is thin to absent in the Right panels with an average interval of 1.9 m when present. This unique sandstone geology and deep cover are combined to generate increased seismic frequency and magnitude (see Figure 8).

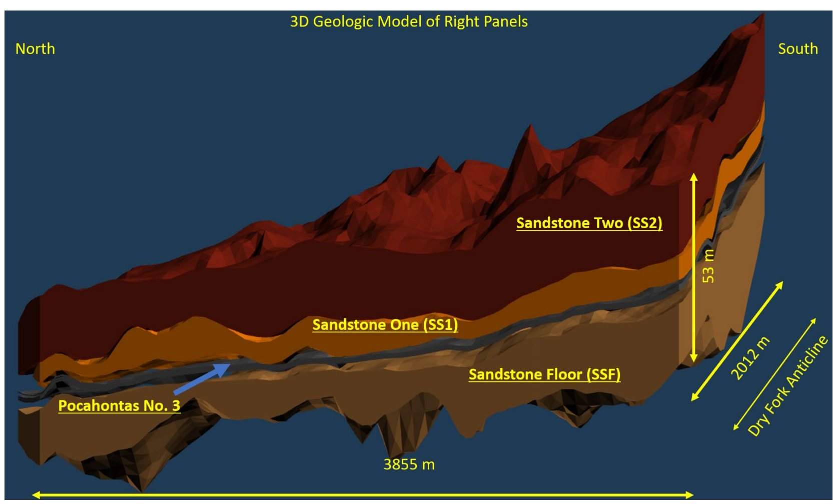


Figure 8. Geologic model of the Right panels.

**Seismicity of the Right Panels**

The deep overburden combined with the sandstone geology led to an increase in seismic event frequency and magnitude with 109 +1.0 magnitude events occurring in the Right panels compared to 64 in the East panels. This difference in the number of events is especially significant given there was 2.5x less longwall footage mined in the Right panels compared to the East panels, but over double the number of +1.0 magnitude events (see Figure 9 and Table 2). The total mine-wide accuracy of the seismic forecasting map since its implementation in 2017 to February of 2022 is summarized in Table 3 (see Table 3).

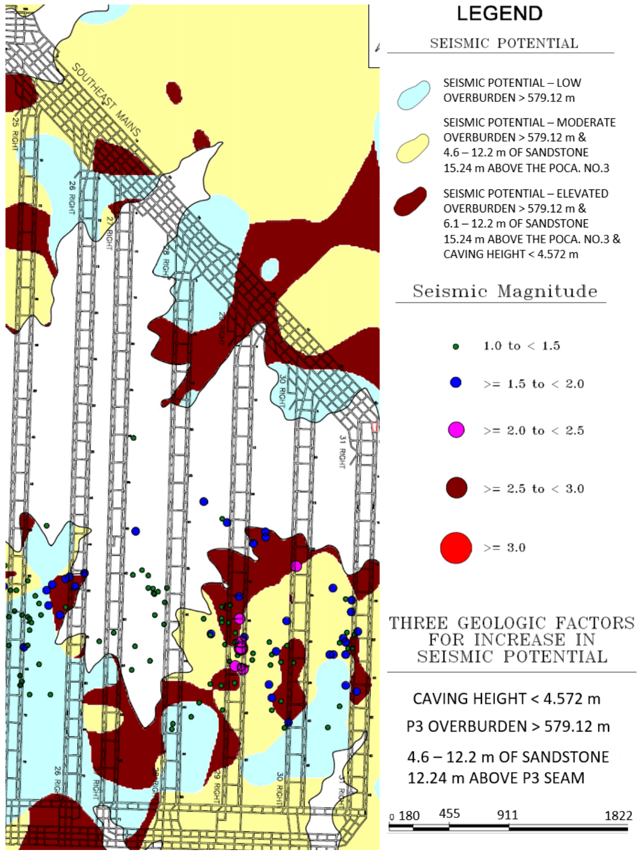

Figure 9. Seismic potential map of the Right panels.

Table 2. Forecasting accuracy of the Right panels.

| Right Panels Seismic Potential Event Accuracy | | | | | | | |
|---|---|---|---|---|---|---|---|
| No Correction | | | | 10% Elevation Bump for Location Error | | | |
| **Event** | **Predicted** | **Total** | **% Correct** | **Event** | **Predicted** | **Total** | **% Correct** |
| **1.0–1.49 ML** | 47 | 68 | 69.1% | **1.0–1.49 ML** | 53 | 68 | 77.9% |
| **1.5–1.99** | 26 | 33 | 78.7% | **1.5–1.99** | 27 | 33 | 81.8% |
| **2.0–2.99** | 7 | 8 | 87.5% | **2.0–2.99** | 7 | 8 | 87.5% |
| **3.0+** | 0 | 0 | - | **3.0+** | 0 | 0 | - |
| **Total** | 80 | 109 | 73.3% | **Total** | 87 | 109 | 79.8% |

**Table 3. Total Seismic Forecast Accuracy**

| Mine-Wide Seismic Potential Event Accuracy Since 2009 | | | | | | | |
|---|---|---|---|---|---|---|---|
| No Correction | | | | 10% Elevation Bump for Location Error | | | |
| **Event** | **Predicted** | **Total** | **% Correct** | **Event** | **Predicted** | **Total** | **% Correct** |
| **M1** | 147 | 243 | 60.4% | **M1** | 189 | 243 | 77.7% |
| **M1.5** | 62 | 102 | 60.7% | **M1.5** | 82 | 102 | 80.3% |
| **M2** | 15 | 25 | 60.0% | **M2** | 19 | 25 | 76.0% |
| **M3** | 2 | 2 | 100.0% | **M3** | 2 | 2 | 100.0% |
| **Total** | 226 | 372 | 60.7% | **Total** | 292 | 372 | 78.4% |

## Future Mining

The seismic forecasting approach used at the mine considered in this study is based on the historical global mining design of 213-m-wide longwall panels. The mine plans to change the mine design and widen the longwall panels to a 305-m-wide panel in a single panel district method with a 61-m barrier of coal between each district. The proposed longwall design change would change the parameters of the three criteria. Due to the increased longwall width, the forecast criteria parameters would change due to increased stresses higher into the roof strata, but the actual upper limits would be unknown due to the lack of history with the design change. Modeling is essential to estimate the forecasting parameters based on the new design change and adjust the forecasting map going into the future (Khademian et al., 2018).

## Discussion

Although the overall accuracy of these criteria for the past mining-induced seismic events is near 80%, there have been noticeable differences in the districts that have been mined thus far since the development of the forecasting approach. Aside from the simple increase in accuracy for the Right panels, it has been observed that the Right panel districts had an absence of seismic activity for the first few panels in each district. The East panels observed seismic activity in the first or second panel, which was not the case in the previously mined Right panel districts. This could be attributed to the change in mining direction, an increase in sandstone thickness near the recovery rooms, or any number of other slight changes to the geologic and geometric characteristics of the districts.

Past observations have shown that there are both geological and mine design parameters that can increase the likelihood and magnitude of seismic events. Some of these characteristics include strong roof and floor, faults, increased depth of cover, rapid changes in topography, and coal properties, although it has been previously postulated that any coal can facilitate seismic activity. As for mine design, factors leading to an increase in seismic activity and magnitude include residual strength of pillars, mining height, formation, amount of gob near active mining, mining rates, and support utilization.

Another interesting outcome of the effort in this study is that it appears that large magnitude events can reasonably be characterized by the three geologic seismic forecasting parameters, whereas the smaller magnitude events might be more influenced by the numerous other parameters leading to mining-induced seismicity. Most of the emphasis in this study has been on the location capability of the seismic system, yet the geological characterization, topography, and mining geometry can also account for some location error. The geological setting is based on modeling between data points, so there could be some relocation of events relative to the sandstone and caving height. The mining geometry is an average of the actual mined geometry, and both the mining height and entry and pillar dimensions could increase the accuracy of this method. Finally, the topography relative to mining location could also explain some of the limitation in the ability of these three characteristics to identify areas of increased seismic activity and severity.

The overall ability to optimize this type of evaluation for seismic potential is the idea that seismic sensor locations must be considered when identifying the deployment locations. As shown, the ideal location of sensors, at or very near seam level, proved impractical at best if not distracting to the overall goal of identifying areas of increased seismic potential. The accuracy of the forecasting map for events 1.0ML and above is between 60.7%–78.4% since the beginning of installing the first seismic system in 2009. The original accuracy of correctly forecasting seismic events of 1.0 ML or greater based historical data from the first paper (Van Dyke et al., 2017) was 89% when accounting the 91 m accuracy buffer. In comparison, the accuracy of forecasting seismic events 10. ML and above that have occurred since publishing the first paper in 2016 is 75.7% correct when incorporating a stricter 58 m buffer.

## Conclusions

- Large mining-induced seismic events create hazards above and below ground. In-mine fires, damage to ventilation controls and injures to mining personnel can result as well as damage to water wells and personal property above ground.
- Since the publishing of the seismic forecasting map in 2017, the map forecasted 75% of 1.0 ML or above events (when accounting for elevation error) in previously unmined areas.
- The seismic forecasting map achieved an overall accuracy of 78.4% mine-wide (when accounting for elevation error) since the installation of the seismic system in 2009.

- The accuracy of the seismic forecasting map increases as the magnitude of events increases. 79.8% of 1.5 ML or greater events were forecasted correctly (when accounting for elevation error) since the installation of the seismic system.
- The seismic forecasting map allows the mine to decide to avoid or appropriately plan to mine high risk seismic areas.

**Acknowledgment**

We wish to thank Coronado Global Resources Inc. for assistance and sharing of data to make this manuscript possible.

**Disclaimer**

The findings and conclusions in this report are those of the authors and do not necessarily represent the official position of the National Institute for Occupational Safety and Health, Centers for Disease Control and Prevention (CDC).

## References

Khademian, Z. (2018). Computational framework for studying seismicity induced by rock engineering activities. Colorado School of Mines. Retrieved from https://hdl.handle.net/11124/172313

Su, Daniel W.H.; Hasenfus, G.J.; Stull, L.A. (2014). Ground Control Design Considerations for Reducing Longwall Induced Stress and Seismicity Associated with Massive Sandstone under Deep Cover. *Proceedings of the 33rd International Conference on Ground Control in Mining.*

Van Dyke, Mark A.; Su, Wen H.; Wickline, Joe (2017). Evaluation of Seismic Potential in a Longwall Mine with Massive Sandstone Roof under Deep Overburden. *Proceedings of the 36th International Conference on Ground Control in Mining*.

Van Dyke, Mark A.; Klemetti, Ted M.; Wickline, Joe; Beale, Jake. (2022). Forecasting Seismic Potential in a Longwall Coal Mine. *Proceedings of the Rockbursts and Seismicity in Mines.* April, RaSiM 10.

Withers, M., Aster, R., Young, C., Beiriger, J., Harris, M., Moore, S., Trujillo, J., 1998, A comparison of select trigger algorithms for automated global seismic phase and event detection: Bulletin of the Seismological Society of America, 88, 95–106.